12-13-2023

SARS-CoV-2 Receptor-Binding Domain-Based Mucosal COVID-19 Vaccines

Melissa L. Palacios

SARS-CoV-2 Receptor-Binding Domain-Based Mucosal COVID-19 Vaccines

by

Melissa Palacios

Under the Direction of Lanying Du, Ph.D.

A Thesis Submitted in Partial Fulfillment of the Requirements for the Degree of

Master of Interdisciplinary Studies

in the Institute for Biomedical Sciences

Georgia State University

2023

ABSTRACT

Severe acute respiratory syndrome coronavirus-2 (SARS-CoV-2) outbreak originating in Wuhan, China in late 2019, declared a pandemic in March 2020 by the World Health Organization, and led to widespread hospitalizations and deaths, prompting a global shutdown. As time progressed, variants emerged, and a solution was needed to prevent the spread. Vaccines and therapeutics were developed, but current vaccines are not able to neutralize all variants and do not have the capability to induce effective mucosal immunity. This study investigates two proteins targeting the receptor-binding domain of the wild-type strain and Omicron variant that are glycosylated and tagged with the Fc portion of human IgG. Three vaccine groups are studied and administered intranasally to induce local and systemic immunity. The findings show that both protein vaccines and their prime-boost vaccination induce high-level titers of specific antibodies with a balanced IgG1/IgG2 level, which could have the potential to be good vaccine candidates.

INDEX WORDS: SARS-CoV-2, COVID-19, Receptor Binding Domain, Mucosal Vaccines

SARS-CoV-2 Receptor-Binding Domain-Based Mucosal COVID-19 Vaccines

by

Melissa Palacios

Committee Chair: Dr. Lanying Du

Committee: Dr. Baozhong Wang

Electronic Version Approved:

Office of Academic Assistance – Graduate Programs

Institute for Biomedical Sciences

Georgia State University

October 2023

DEDICATION

I would like to dedicate my thesis to my loving, supportive family who have helped me throughout my journey. Nothing would be possible without the encouragement of my parents, siblings, uncle, and niece. All of this is done for you. Thank you especially to my parents for making your life in an unknown country.

I would like to thank my partner. Thank you for being my shoulder to lean on during this time and keep pushing me to be a better person.

To my friends: thank you for always giving me words of wisdom and advice when I need it.

Lastly, in memory of Brenda Cisneros: thanks for helping me get into graduate school and always being a great best friend.

ACKNOWLEDGEMENTS

I would like to express my gratitude to my PI and committee chair Dr. Lanying Du for allowing me to be involved your lab. Thank you for your guidance, feedback, and support throughout this research process. Thank you to my committee member Dr. Baozhong Wang. I appreciate your support, time, and expertise. I appreciate you both for providing feedback and enhancing the quality of the work.

Thank you to my mentor Dr. Xiaoqing Guan. I appreciate your expertise and patience in helping me understand the topic with deeper knowledge.

Lastly, thank you to all my lab members for aiding me through this entire process. I would have not it without all your support and assistance.

TABLE OF CONTENTS

LIST OF TABLES

LIST OF FIGURES

1. INTRODUCTION

Coronavirus Disease 2019 (COVID-19), caused by severe acute respiratory syndrome coronavirus-2 (SARS-CoV-2), has led to a worldwide health emergency. According to the World Health Organization, there have been a total of at least 6.9 million deaths among the 771 million confirmed cases of COVID-19 as of November 08,2023 (1). As time progresses, the virus is mutating, and vaccines are needed to keep up with the emerging variants. Current vaccines are not able to induce, or elicit low, neutralizing antibodies against newly emerging variants.

1.1 SARS-CoV-2 Classification

SARS-CoV-2 is a part of the same genus as SARS-CoV and Middle East respiratory syndrome coronavirus (MERS-CoV), which is *Betacoronavirus* and belongs to the *Coronavirinae* subfamily, *Coronaviridae* family, and *Nidovirales* order (2). The genome of SARS-CoV-2 is 79% identical to the SARS-CoV sequence and 50% identical to the MERS-CoV sequence (3). The shared similarities and differences of the genetic sequences for each of the viruses allowed for the identification of the cell entry receptors (3).

1.2 SARS-CoV-2 Structure

SARS-CoV-2 is composed of a large positive-stranded RNA genome which encodes four structural proteins: spike (S), envelope (E), membrane (M), and nucleocapsid (N) (4). The S protein consists of two subunits, S1 and S2, each forming a trimer (4). S1 is composed of N-terminal domain (NTD) and the receptor-binding domain (RBD), while S2 is composed of heptad repeat 1 (HR1) and heptad repeat 2 (HR2) (5).

1.3 S Protein Function

The S protein plays a major role in viral infection (6). Viral infection starts with the S1 subunit, specifically, the RBD binds to the host cellular receptor angiotensin-converting enzyme 2 (ACE2) (4). The S2 protein facilitates membrane fusion (4). Not only does the S protein enable viral entry, but it also promotes adhesion of the infected cells with adjacent non-infected cells, thereby increasing the viral load (4).

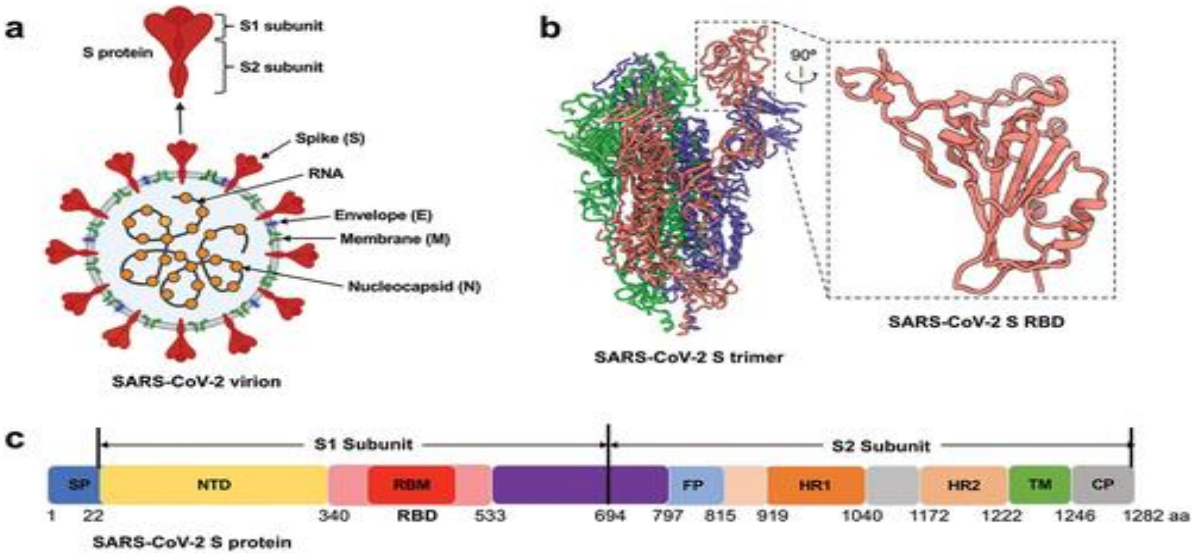

Figure 1: Virion and S Protein Structure of SARS-CoV-2 (7).
A) Represents the structure of virion; B) Display of the crystallized structure of the spike (S) protein emphasizing the RBD portion of the S protein; C) Display of the entire S protein genome.

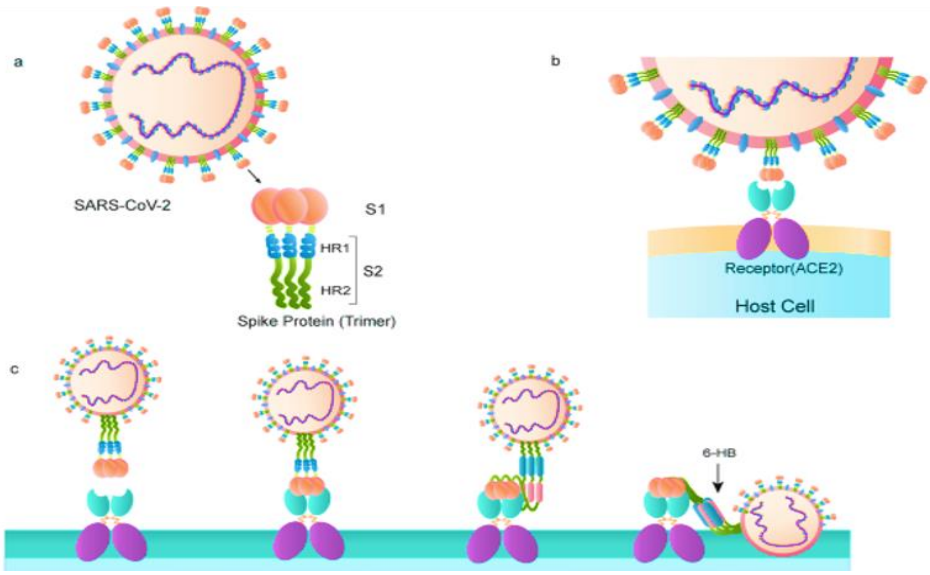

Figure 2: Display of SARS-CoV-2-Spike Protein in Different Conformations (8).
A) Structure of spike (S) protein; B) Virus binding to host cell; C) Attachment of virus to host cell.

1.4 Life Cycle of SARS-CoV-2

The virus enters through the respiratory tract, where the S1 subunit binds to the ACE2 receptor on the respiratory epithelium (9). S2 allows for fusion of membrane by allowing entry into the host cell with the aid of host factors, including cell surface serine protease TMPRSS2 (10). Once the virus has entered the host cell, the RNA is released and uncoated, allowing for the translation of two large open reading frames (ORF), ORF1a and ORF1b (10). The polyproteins translated from the ORFs, pp1a and pp1ab, are cleaved by proteases from the non-structural protein (NSP) 3 and NSP5, forming 16 NSPs, which constitutes the replication-transcription complexes (RTCs) (11).

Double membrane vesicles (DMVs) are formed by the NSPs through reshaping the cell membrane, which then join with the endoplasmic reticulum (ER) (12). RNA replication occurs within the DMVs, and the RNA exits through the transmembrane pores to either go to translation or assembly (12). Translated structural proteins move to the ER membrane and

progress through the ER-to-Golgi intermediate compartment (ERGIC) (12). The RNA positive strand, wrapped by the N protein, undergoes assembly with the structural proteins to form the virion, and eventually bud into the lumen at ERGIC to be released by the infected cell via exocytosis (12).

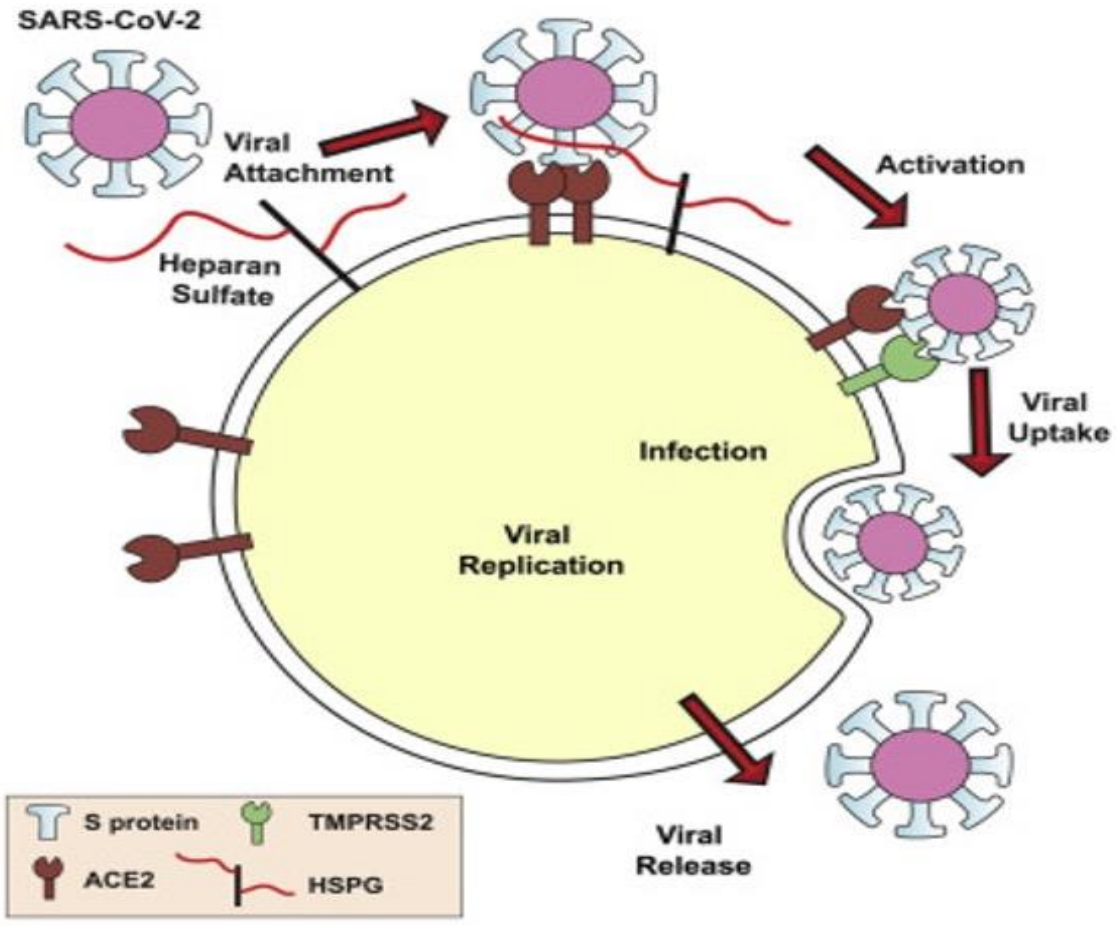

Figure 3: Life Cycle of SARS-CoV-2 (13).

1.5 COVID-19 Variants

Through the circulation of SARS-CoV-2 among the population, the genome undergoes consistent mutations. Mutations arise from the discontinuous transcription of the coronavirus, resulting in high rates of recombination, insertions, deletions, and/or point mutations (14). Co-infection of the host cell by two RNA viruses increases the chance of the polymerase switching the genome between the two RNA strands during replication and generating a new genome (14). Initially, when SARS-CoV-2 was first circulating, it was known to have limited adaptation and phenotypic change, and around October of 2020, the genome started to have heavy mutations and variants started to emerge (14).

Since the start of the pandemic, there have been many variants of concern (VOCs) which include Alpha, Beta, Gamma, Delta, and Omicron (14). Omicron exhibits a faster doubling time at 1.2 days, while Beta and Delta are 1.7 and 1.5 days, respectively (15). Omicron also has a shorter incubation period at 3 days, in contrast to the 5 days observed by the wild-type (15). The success of these VOCs can be attributed to various factors, including varying severity of disease, immune evasion, sensitivity to therapeutics, transmission advantages due to changes in the S protein, optimization of furin-mediated cleavage, and more (14).

Figure 4: Timeline of Variants that Emerged (16).

1.6 COVID-19 Spread

The respiratory virus primarily transmitted through close contact with an infected individual (17). An infected individual may release small liquid particles containing virus from the mouth or nose by coughing, sneezing, speaking, singing, or breathing (17). Non-infected individuals may encounter the particles within a short range of the infected individual entering the eyes, nose, or mouth to become infected (17). Another way the virus can spread is through poorly ventilated or crowded places since the aerosols can be suspended in the air for a longer time and travel further (17). A person may come in contact by touching a contaminated surface or object followed by touching their eyes, nose, or mouth (17).

The basic reproduction number, R_0, represents the number of infections that a single infection can produce, and an individual infected with the wild-type strain can infect 2-4 people (18). With the emergence of variants, the R_0 has increased; the R_0 for the Delta strain was 5-8 days and for Omicron it is approximately 10 days (15). In the United States, the case fatality is reported to be 1.1% (19).

1.7 Vaccine Development Against COVID-19

To mitigate the spread of COVID-19, various measures must be implemented, such as creating herd immunity through widespread vaccination. As of August 2021, there are 21 vaccines that are approved for emergency use worldwide (20). Popular and successful targets for the vaccine include S protein or the S1 domain, which has the RBD portion to prevent viral entry into host cells (21).

In the United States, there are currently three vaccines approved for use: two mRNA vaccines, by Pfizer-BioNTech and Moderna, and a protein subunit vaccine by Novavax (22). The

mRNA vaccine technology, utilizing lipid nanoparticles (LNPs), delivers a nucleic acid molecule that encodes a protein to the host cell, which makes the protein and elicits an immune response against that protein (23). When Pfizer and Moderna both released their vaccines, it was at a 95% efficacy rate. After the emergence of the variants, the efficacy of the vaccines decreased (15). For the Pfizer-BioNTech mRNA vaccine, the efficacy dropped to 63.5% for the Delta variant and 34-37% for the Omicron variant (15). For the Moderna mRNA vaccine, the efficacy dropped to 62.5% for the Delta variant and 30.4% for the Omicron variant. In result of the low efficacy against the emergent strains, the formulations for the vaccines changed to keep up with the current circulating strains (24).

1.8 Alternative Route for Vaccine

The nasal-associated lymphoid tissue (NALT), in the nasal cavity, contains a dense amount of lymphatic tissue (25). Immunoglobulin A (IgA) constitutes about 15% of total immunoglobulins and is secreted in higher percentages in the nasal cavity compared to serum (25). IgA plays a crucial role in creating mucosal immunity, and approximately 80% of the immune cells are in the mucosal area (25). Since the route of infection for SARS-CoV-2 starts in the respiratory area, the first line of defense should be created in the respiratory area.

There are current studies focusing on the mucosal route, in specific using the adenovirus vector delivery system and subunit vaccines. These vaccines have the potential to produce a strong immune response against COVID-19 such as creating mucosal IgA antibodies and protecting the upper and lower respiratory tract against infection from the virus (26, 27).

1.9 Current Study

For this study, the focus is a subunit intranasal vaccine administered in a series. The purpose is to establish a first line of defense by inducing mucosal IgA antibodies and overall neutralizing antibodies against previous and emerging strains of SARS-CoV-2. Because the first step to viral replication is the binding of RBD to ACE2, it is important to target vaccines and therapeutics to the S protein and more importantly to the RBD (7, 5). Previous studies observed antibody neutralization of the viral RBD elicits a stronger reaction than antibodies that target other regions of the S protein (5). The vaccine created was based on previous studies; residue sites 519 and 521 were glycosylated for the mutant RBD subunit vaccine and an Fc fragment of human immunoglobin G (IgG) was attached for an effective vehicle for the delivery intranasally (7, 28). The results within these studies showed that the subunit vaccines with glycosylation and addition of the Fc portion of the human IgG induced robust systemic immune responses as well as high mucosal IgA titers with an intranasal vaccine. The published papers provided the foundation of this study to create a wild-type RBD and an Omicron variant RBD (XBB-RBD) that are glycosylated and tagged with the Fc portion of human IgG.

2. Materials and Methods for Protein Construct

2.1 Construct of Vaccine

The plasmid structures for both the glycosylated wild-type RBD and mutant RBD from Omicron XBB1.5 variant, SARS2-CoV-2 RBD-Fc-Gly and XBB-RBD-Fc-Gly (hereinafter SARS-CoV-2 wild-type-RBD and XBB-RBD, respectively), and the primers were designed by Dr. Lanying Du. The DNA template used for SARS-CoV-2 wild-type-RBD for PCR was pCA-nCOV-RBD (encoding the original RBD), and the primers used were XbaI-tPA-plenti-F1 and SARS2-S524-Gly-R. The

DNA template used for SARS-CoV-2 XBB-RBD (encoding the XBB1.5-RBD) for PCR was pUC-XBB-RBD-Fd and the primers used were XbaI-tPA-plenti-F2 and XBB-S524-Gly-R. The proteins are glycosylated at the 519 and 521 residues of the RBD sequence and attached to the Fc domain of human IgG.

2.2 Polymerase Chain Reaction (PCR)

The DNA template pCA-nCOV-RBD was used for amplification by using polymerase chain reaction (PCR) to obtain the SARS-CoV-2 wild-type-RBD sequence. The forward primer used was XbaI-tPA-plenti-F1 and the reverse primer used was SARS2-S524-Gly-R.

Similarly, the DNA template pUC-XBB-RBD-Fd was used for PCR amplification to produce the SARS-CoV-2 XBB-RBD sequence. The forward primer used is XbaI-tPA-plenti-F2 and the reverse primer used is XBB-S524-Gly-R.

For both reactions, a 50 μl reaction was done with the following components and amounts used:

Component:	Amount (μl or ng):
DNA Template	10 ng
Primers	1 μl + 1 μl
Master Mix	25 μl
H_2O	Up to 50 μl

Table 1: Components and Amounts Used for PCR.

The protocol listed below was the program used for PCR:

Step	Temperature (°C)	Time	
Initial Denaturation	95°C	3 minutes	
Denaturation	95°C	30 seconds	Repeated for 30 cycles.
Annealing	55°C	30 seconds	
Extension	72°C	3 minutes	
Final Extension	72°C	5 minutes	
Holding	12°C	∞	

Table 2: Program Used for PCR.

2.3 Digestion for Large Size Vector

A restriction enzyme double digestion was done with the protocol using a 50 μl reaction to isolate the large size vector.

Component:	Amount (μl or μg):
DNA	1 μg
10X NEBuffer	5 μl
Restriction Enzyme XBaI	2.5 μl
Restriction Enzyme BamHI	2.5 μl
Nuclease-Free Water	Up to 50 μl

Table 3: Components and Amounts Used for Digestion.

The following reaction was incubated at 37°C for 15 minutes and a 1% Agarose DNA gel was used. The larger fragment was collected by extracting the DNA from the gel using QIAquick Gel Extraction Kit (250).

2.4 Ligation of Large Size Vector and Insertion of PCR Product

Seamless Cloning Kit was utilized to ligate the PCR fragments into the large-sized vector obtained from the digestion reaction. Each sequence underwent ligation in a 20 μl reaction and incubated for 30 minutes at room temperature.

Component:	Amount (μl or ng):
T4 DNA Ligase Buffer (10X)	2 μl
Vector DNA	50 ng
Insert DNA	37.5 ng
Nuclease-Free Water	Up to 20 μl
T4 DNA Ligase	1 μl

Table 4: Components and Amounts Used for Ligation.

2.5 Plasmid Transformation

Competent cells from the laboratory stock were retrieved from -80°C and thawed on ice. Approximately 50 ng (1-2 μl) of plasmid was added into the cells and placed on ice for 30

minutes. The cells underwent a 90-second heat shock at 42°C, followed by immediate placement on ice for 3 minutes. Subsequently, 1 mL of room temperature Lysogeny Broth (LB) was added, and the mixture was incubated in a 37°C shaker between 30-50 minutes. Lastly, about 50 μl of the treated cells were spread onto an Agar plate containing ampicillin and incubated at 37°C.

2.6 Mini Extraction Kit

A colony from the agar plate containing ampicillin was transferred into 10 mL of LB with 10 μl of ampicillin and incubated in a 37°C shaker overnight. The QIAprep Spin Miniprep Kit (Qiagen) protocol was used to extract the plasmid. The nanodrop was used to measure the concentration.

2.7 Plasmid Digestion

To verify the plasmids, digestions were done with the following components and amounts in a 50 μl reaction and incubated in a 37°C water bath for 2 hours.

Component:	Amount (μl or μg):
10X Fast Digestive Buffer	5 μl
Plasmid	5 μg
Restriction Enzyme XbaI	2.5 μl
Restriction Enzyme BamHI	2.5 μl
H_2O	Up to 50 μl

Table 5: Components and Amounts Used for Plasmid Digestion.

2.8 Gel Electrophoresis

A 1% DNA gel, prepared using agarose and Tris-acetate-EDTA (TAE) buffer, was used to run the plasmid digestions. The electrophoresis was carried out at 80V for 1 hour.

2.9 Maxi Extraction Kit

Bacterial stock in glycerol is stored in -80°C. A mini culture was initiated with 10 mL of LB, 10 μl of ampicillin, and 10 μl of thawed bacterial stock. The mini culture was incubated in a 37°C shaker for 4 hours. Following this, the mini culture was transferred into 1L of LB with 1 mL of ampicillin and incubated overnight in the 37°C shaker. The QIAGEN Plasmid, Mini, Midi and Maxi Kits (Qiagen) protocol was followed. Several critical steps from the Qiagen protocol for Maxi Kit were altered to enhance the plasmid yield and are listed below. All other steps followed the protocol.

Step 5: Centrifuged at 10,000 x g for 30 minutes at 4°C.

Step 9: Elute DNA with 20 mL of Buffer QF.

Step 10: Precipitate DNA by adding 14 mL of room temperature isopropanol.

Step 11: Centrifuge at 12,000 x g for 10 minutes.

The nanodrop was used to measure the concentration of plasmids.

2.10 Protein Expression

Lab stock of HEK (Human Embryonic Kidney) 293F cells underwent transfection with the plasmids SARS-CoV-2 wild-type RBD and XBB-RBD, using Polyethylenimine (PEI) as the transfection reagent. The cells were cultured at 37°C with 5% CO_2 in ESF serum-free medium (CSF). After 96 hours, the supernatant was collected by centrifuging the 293F cells. Since the proteins are Fc-tagged, N-protein A beads were added to the supernatant and incubated at 4°C on a shaker overnight. The following day the supernatant was purified for each protein, which was concentrated and washed with 1X concentration of phosphate-buffered saline (PBS).

2.11 SDS-PAGE (Sodium Dodecyl Sulfate-Polyacrylamide Gel Electrophoresis)

The purified proteins were separated on two 10% gels, each serving a distinct purpose —one gel for Coomassie staining and the other for Western Blot analysis. In both gels, a non-boiled and boiled sample were added for each protein. The boiled samples were prepared by adding BME (beta-mercaptoethanol) to the 4X Laemmli Sample Buffer (LSB) at a 1:4 dilution. A 30 μl reaction was prepared for each sample with the following components:

Component (Non-Boiled)	Amount (μl or μg)
Protein	2.5 μg
4X LSB	7.5 μl
ddH_2O	Up to 30 μl

Table 6: Components and Amounts for Non-Boiled Samples for Coomassie Stain.

Component (Boiled)	Amount (μl or μg)
Protein	2.5 μg
4X LSB + BME	7.5 μl
ddH_2O	Up to 30 μl

Table 7: Components and Amounts for Boiled Samples for Coomassie Stain.

Component (Non-Boiled)	Amount (μl or μg)
Protein	0.5 μg
4X LSB	7.5 μl
ddH_2O	Up to 30 μl

Table 8: Components and Amounts for Non-Boiled Samples for Western Blot.
An additional 120 μl of ddH_2O was added to have a 1:5 ratio of the non-boiled sample for Western Blot.

Component (Boiled)	Amount (μl or μg)
Protein	1 μg
4X LSB + BME	7.5 μl
ddH_2O	Up to 30 μl

Table 9: Components and Amounts for Boiled Samples for Western Blot.

The electrophoresis was conducted at 120V, 3.00A, and 300W for 1 hour 20 minutes.

2.1.1 Coomassie Stain

Following the SDS-PAGE, the gel underwent multiple washes with double distilled water (ddH_2O). The gel was immersed in a container with Coomassie blue staining and incubated on a shaker for 1 hour. After staining, the gel was then washed with ddH_2O and was left immersed in ddH_2O overnight to eliminate any residual stain.

2.1.2 Western Blot

The SDS-PAGE Gel was loaded into the gel holder cassette, which included the gel, membrane, filter papers, and sponges. This cassette was inserted into the electrode assembly and placed in the tank filled with transfer buffer. The electrophoresis was conducted overnight at 30V, 3.00A, 300W. The following day the membrane was blocked with 5% fat-free milk in PBS containing 0.05% Tween 20 (PBST) for 1 hour on a shaker. The membrane was washed with PBST 3 times, each for 5 minutes on a rotary shaker. Serum from a mouse intramuscularly immunized with glycosylated SARS-CoV-2 Delta-RBD was used as the primary antibody at a 1:10,000 ratio in 2% fat-free milk for 1 hour on the rotary shaker. The membrane was washed 5 times for 5 minutes each with PBST on the rotary shaker. The secondary antibody used was horseradish peroxidase (HRP)-conjugated goat anti-Mouse IgG (H+L) (Invitrogen, #31430) at a 1:10,000 ratio in 2% fat-free milk in PBST, and the membrane was incubated for one hour on the rotary shaker. The membrane was washed five times for five minutes each with PBST on the rotary shaker.

To visualize the results, a 1:1 mixture of Clarity Western ECL Substrate Lumino/Enhancer Solution and Clarity Western ECL Substrate Peroxide Solution was pipetted onto the membrane for 5 minutes.

3. Methods and Materials for the Vaccination of BALB/c Mice

3.1 Trial Run of Mouse Vaccination

In the trial run involving BALB/c female mice aged 6-8 weeks, combinations of proteins were evaluated to determine which ones would be utilized for the long-term study. This resulted in six groups, with two mice allocated to each group. The trial schedule comprised of two vaccinations, a prime and a boost, with a 2-week gap in between, followed by collecting serum. Ethical euthanasia was performed to collect the bronchoalveolar lavage (BAL) fluid. The 6 groups used were:

1. Prime & boost: SARS-CoV-2 wild-type-RBD
2. Prime & boost: SARS-CoV-2 XBB-RBD
3. Prime: XBB-RBD & Boost: Wild-type-RBD
4. Prime: Wild-type-RBD & Boost: XBB-RBD
5. Prime & Boost: A mixture of wild-type-RBD and XBB-RBD
6. Control group using PBS

Each mouse was vaccinated intranasally with 20 μl, 10 μl inserted in each nostril using a 10 μl pipet.

3.2 Components of Vaccines for Trial Run

For vaccines containing a single protein, 5 μg of the protein was combined with PBS (to a total volume of 15 μl). Additionally, Poly (I:C) (Polyinosinic:polycytidylic acid) was used as the adjuvant at a concentration of 2 $\mu g/\mu l$ concentration, derived from a 2 mg/ml stock concentration, resulting in the utilization of 5 μl. Vaccines with a combination of two proteins

used 2.5 μg of each protein combined with PBS (to a total volume of 15 μl) and 5 μl of Poly (I:C). The total volume of each vaccine is 20 μl per mice.

3.3 Long-term Vaccine Study

For the long-term vaccine study, a prime vaccination is followed by two booster vaccinations. The selected vaccine combinations for the full study are as follows (Figure 5):

1. Prime, boost, & boost: SARS-CoV-2 wild-type-RBD (WT-RBD)
2. Prime, boost, & boost: SARS-CoV-2 XBB-RBD (XBB-RBD)
3. Prime: XBB-RBD, Boost: Wild-type-RBD (WT-RBD), & Boost: Wild-type-RBD (WT-RBD)
4. Control group using PBS

Each group is comprised of 5 BALB/c female mice aged 6-8 weeks. Intranasal vaccination was performed with 20 μl, delivering 10 μl into each nostril using a 10 μl pipet. The first vaccination serves as the prime vaccine. After 10 days, serum samples were collected. Three weeks following the prime vaccine, the first booster was administered. Serum was collected 10 days following the first booster. Three weeks after the first boost, a final booster was administered. Serum was collected 10 days following the final booster.

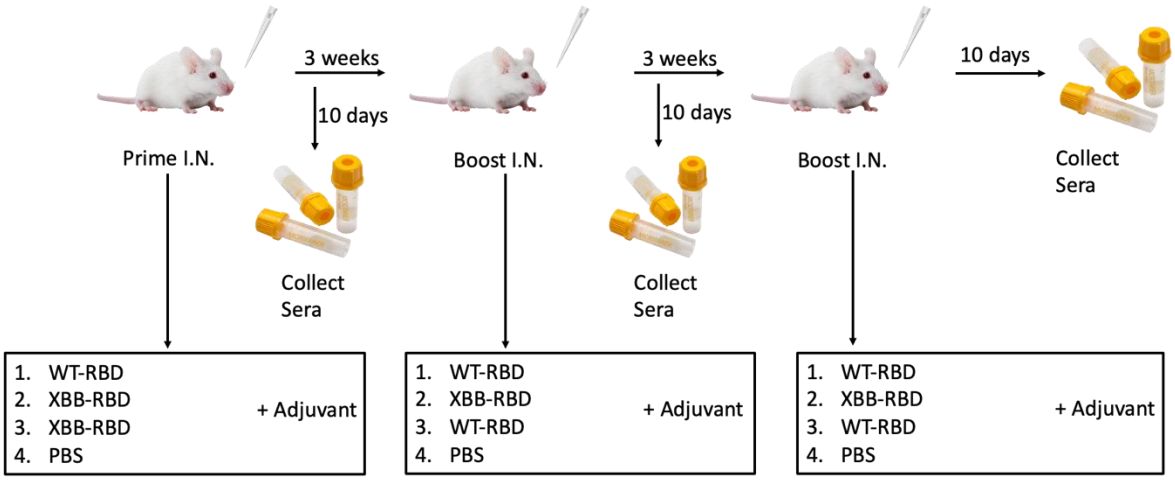

Figure 5: Mouse Vaccination Schedule.

3.4 Components of Vaccines for Full Vaccine Run

10 μg of each protein was combined with PBS (to a total volume of 15 μl) and 5 μl of Poly (I:C) adjuvant was added, resulting in a total volume of 20 μl per mouse.

3.5 ELISAs

3.5.1 ELISA to Test Binding for the hACE2 Receptor

The binding of the proteins to the hACE2 receptor was tested using ELISA. In a single plate, nine wells were allocated, three for each protein (SARS-CoV-2 wild-type-RBD and XBB-RBD), and three for the PBS control. Each well was coated with 2 $\mu g/mL$ of protein or PBS with coating buffer, and the plates were incubated at 4°C overnight. Afterward, the plate was washed three times with PBST, then blocked with 2% fat-free milk in PBST and incubated at 37°C for 1 hour. Following another three washes with PBST, 5 $\mu g/mL$ of a hACE2 protein from a laboratory stock, diluted in 0.5% fat-free milk in PBST, was added to three wells per protein or PBS and incubated for 2 hours at 37°C. The plate was washed six times with PBST, and the primary antibody (anti-goat-hACE2) (R&D Systems, AF933) was added at a 1:1,000 dilution ratio

in 0.5% fat-free milk in PBST and incubated for 1 hour at 37°C. After six additional washes with PBST, the secondary antibody, rabbit-anti-goat IgG-HRP (Acbam, ab6741), was added at a 1:10,000 dilution in 0.5% fat-free milk in PBST and incubated for 1 hour at 37°C. The plate was washed six more times with PBST, and further incubated with TMB (3,3',5,5'-tetra-methylbenzidine) (Sigma-Aldrich). The reaction was stopped by the addition of 1 N H_2SO_4, and the absorbance at 450 nm (A450) was measured using the Cytation 7 Microplate Multi-Mode Reader (BioTek Instruments).

3.5.2 ELISA to Test Binding for Monoclonal Antibodies

The binding of the proteins to the monoclonal antibodies was tested using ELISA. For each protein and PBS, 12 wells were coated with coating buffer and 1 $\mu g/mL$ of protein or PBS, totaling 36 wells and incubated overnight at 4°C. The following day, the plates were washed three times with PBST; 2% fat-free milk in PBST was added and incubated at 37°C for 1 hour. After three additional washes with PBST, two monoclonal antibodies, anti-spike protein (RBD) (Absolute Antibody, Ab02019-10.0) and anti-spike protein (RBD) (Absolute Antibody, Ab03065-10.0), were added in triplicates with two different concentrations (5 $\mu g/mL$ and 10 $\mu g/mL$) in 0.5% fat-free milk in PBST and incubated at 37°C for 2 hours. The plates were washed 6 times with PBST, and a 1:1000 ratio of the secondary antibody, mouse anti-human IgG Fc-specific HRP (Invitrogen, #05-4220), was added and incubated at 37°C for 1 hour. Following another six washes with PBST, the plates were further incubated with TMB, and the reaction was stopped by 1 N H_2SO_4. The absorbance was measured using the Cytation 7 Microplate Multi-Mode Reader at the 450 nm (A450) absorbance as described above.

3.5.3 ELISA for Antibody Titers

IgG and subtype antibodies specific to each protein was detected by ELISA. ELISA plates were coated with coating buffer and the respective protein, with each well containing 1 $\mu g/mL$ and incubated overnight at 4°C. For each secondary antibody studied, six plates were coated, three for each protein since there are 20 mouse serum samples. The following day, the plates were washed three times with PBST, and then blocked with 2% fat-free milk in PBST for 1 hour at 37°C, followed by additional 3 washes of PBST.

A serial dilution of the serum was done on separate plates using 0.5% fat-free milk in PBST. Each row of the plate was designated to one mouse, resulting in 20 rows being used (three plates). In the first well for each row (20 total), 98 μl of 0.5% fat-free milk was added, and 90 μl was added to the rest of the wells. For the first well for each row, 2 μl of serum was added, mixed thoroughly, and 30 μl was transferred to following column. This process was repeated until the 11th column. After the thorough mixing of the 11th column, the 30 μl was discarded leaving the 12th column 90 μl of 0.5% PBST to serve as the blank. This serial dilution results in a dilution factor of 3.

From the serial dilution plates, 50 μl was transferred from each well to the ELISA plates that were coated with the respective protein and incubated overnight. The plates were then washed six times with PBST. Depending on the secondary antibody, the ratios varied; 1:20,000 for Goat anti-Mouse IgG (H+L) (Invitrogen, #31430), 1:60,000 for Anti-Mouse IgG (Fab specific) (Sigma, #A9917), 1:8,000 for Goat anti-Mouse IgG1 (Invitrogen, #PA1-74421), and 1:2,000 for Goat anti-Mouse IgG2a (Invitrogen, #M32207). All antibodies were diluted with 0.5% fat-free milk in PBST. The plates were incubated for 1 hour at 37°C and then washed six times with

PBST. The plates were further incubated with TMB, and the reaction was stopped by 1 N H_2SO_4. The absorbance was measured using the Cytation 7 Microplate Multi-Mode Reader at the 450 nm (A450) absorbance, as described above.

4. Results

4.1 Construction of Plasmids

Previous studies demonstrated the development of a subunit vaccine involving the masking of an epitope surrounding residue Asn519 of the RBD portion of the S protein with a glycan probe (28). The glycan probe introduced mutations at residue sites 519 and 521, creating an N-glycosylation site. The resulting mutant RBD protein successfully induced a high titer of neutralizing antibodies against various SARS-CoV-2 variants. Building upon this research, a glycan probe was incorporated, along with an Fc fragment to be used as the vehicle, into both wild-type and mutant RBD protein fragments. The plasmid structures about 640 base pairs (bp) in size were constructed and amplified by PCR, attached to the large size vector fragment of pCA-nCOV-RBD, and transformed with competent cells. The resulting plasmids were verified by gel electrophoresis (Figure 6), confirming the sizes of SARS-CoV-2 wild-type-RBD and SARS-CoV-2 XBB-RBD (XBB1.5 variant).

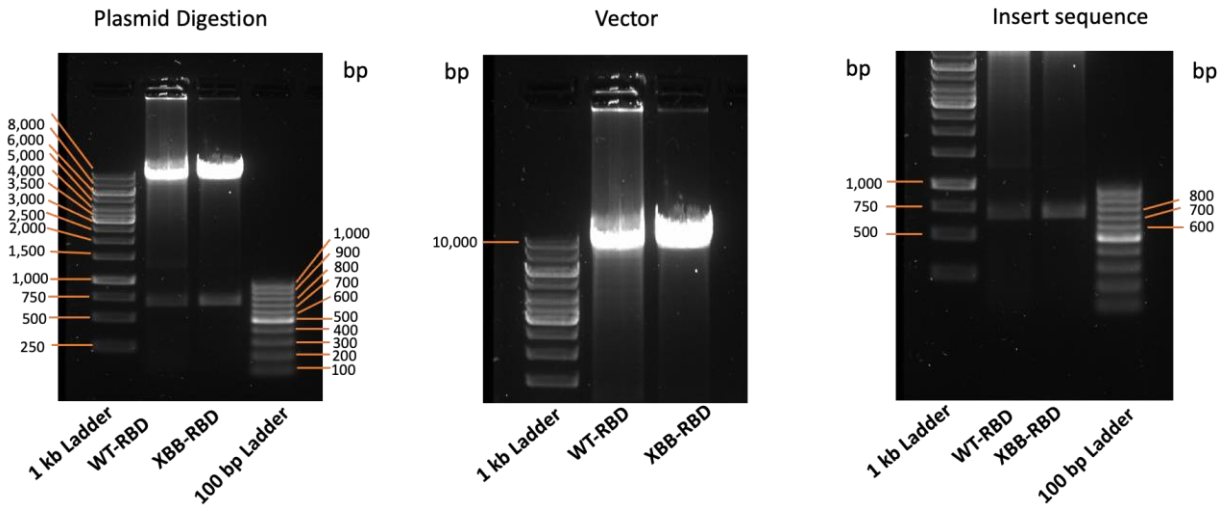

Figure 6: Plasmid Digestion of SARS-CoV-2 Wild-Type-RBD and XBB-RBD.

4.2 Protein Expression

HEK 293F cells were transfected using previously extracted plasmids. These cells serve as an alternative expression system to the prokaryotic expression systems, such as *E. coli* (29). *E. coli* and other prokaryotic expression systems lack specific co-factors-chaperones, and post-translational modifications can cause the protein to lose its function, and therefore the use of mammalian cells can help address these limitations (29). Transfection of HEK 293F cells can yield large amounts, and the resulting proteins were verified by SDS-PAGE Coomassie stain and Western Blot (Figure 7). Both proteins were analyzed in a boiled and non-boiled state. Addition of Fc fragment of IgG to each RBD (wild-type-RBD (WT-RBD) and XBB-RBD) formed a dimer conformation. With the boiling and addition of BME, the S-S bonds are disrupted, and the RBD proteins become monomers. The size of the resulting monomeric and dimeric proteins is between 64 kDa and 148 kDa. Western Blot was used to confirm the protein specific to the RBD, and by doing so the primary antibody used was serum from mice immunized intramuscularly by SARS-CoV-2 Delta-RBD protein. The secondary antibody used was Goat anti-

Mouse IgG (H+L) (Invitrogen, #31430). The results showed the antibodies from the serum bound strongly to the respective RBD proteins whether they were boiled or not, further proving that the protein does bind to SARS-CoV-2 anti-RBD antibodies.

Figure 7: SDS-PAGE Coomassie Stain and Western Blot.

4.3 Characterization of Proteins

The binding of the protein to the host cell receptor (hACE2) was tested to see which protein has a stronger binding affinity. A stronger binding indicates a more robust attachment. Figure 8 exhibited SARS-CoV-2 XBB-RBD having a stronger affinity to the receptor compared to the SARS-CoV-2 WT-RBD (SARS-CoV-2 wild-type-RBD), and the control group using PBS only resulted in background levels.

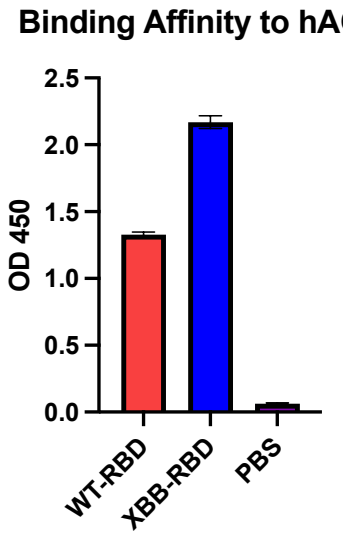

Figure 8: Binding Affinity of Proteins to hACE2 Receptor.
The hACE2 protein at 5 $\mu g/mL$ was used for test.

The binding of the protein was also tested against purified monoclonal antibodies that specifically target the RBD portion of the S protein. Two different monoclonal antibodies were tested at two different concentrations and in both cases, the monoclonal antibodies have a stronger binding affinity to the SARS-CoV-2 wild-type (WT)-RBD protein.

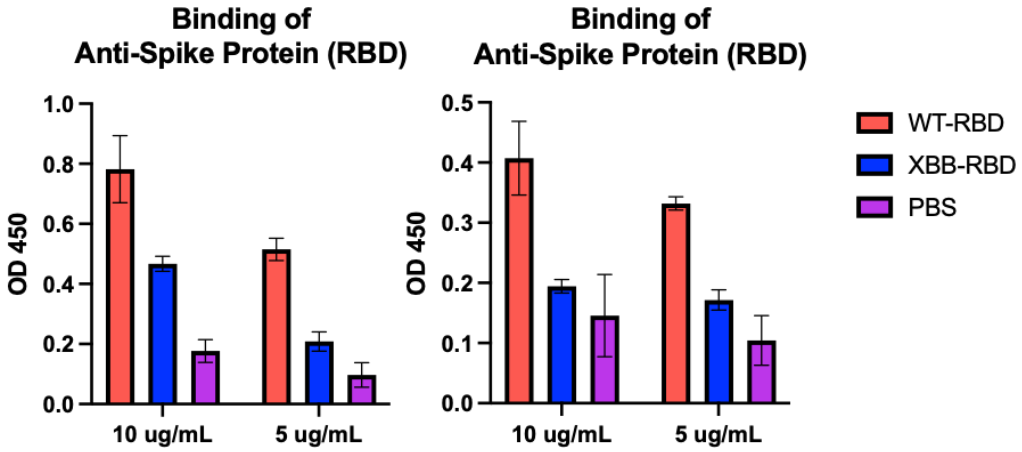

Figure 9: Binding of Proteins to Two Monoclonal Antibodies.
The left graph is displaying Anti-Spike-Protein (RBD) (Absolute Antibody, Ab03065-10.0) monoclonal neutralizing antibody, and the right is displaying Anti-Spike Protein (RBD) (Absolute Antibody, Ab02019-10.0) monoclonal neutralizing antibody.

4.4 Groups Chosen for Vaccine Full Run

The preliminary vaccine trial determined to identify the most effective vaccine groups for the comprehensive study. Analyses of the sera and BAL were done by the lab and determined the optimal groups. The groups chosen: Group 1 – SARS-CoV-2 wild-type-RBD (3 doses), Group 2 – XBB-RBD (3 doses), and Group 3 – a prime vaccination of XBB-RBD followed by two boosts of wild-type-RBD vaccine (see Figure 5 for the detailed immunization and sample collection protocol).

4.5 Titer of IgG and Subtypes

Sera from mice vaccinated with the proteins and PBS were analyzed to assess the immune system's response in producing high levels of protective antibodies. The main immunoglobulin studied is IgG, and out of other isotypes, it is the most abundant in serum (30). Various IgG subtypes were tested, and the first antibody studied was IgG Fab portion. The sera were tested from each collection time point to compare the prime vaccine to the boosters. This comparison aimed to determine whether a booster, or even two, is necessary to induce high levels of IgG (Fab) specific to SARS-CoV-2 wild-type-RBD and XBB-RBD proteins. The use of IgG Fab portion aimed to minimize non-specific binding, considering that the proteins created are tagged with the Fc portion of IgG. Figure 10 shows the comparison of all three sera. Across all graphs, PBS induced a background level of response, while the three protein groups induced high-titer IgG (Fab) levels. The second serum (10B and 10E) induced higher levels than the first serum (10A and 10D). The result from the second booster (10C and 10F) showed a slightly increased titer compared to the first booster.

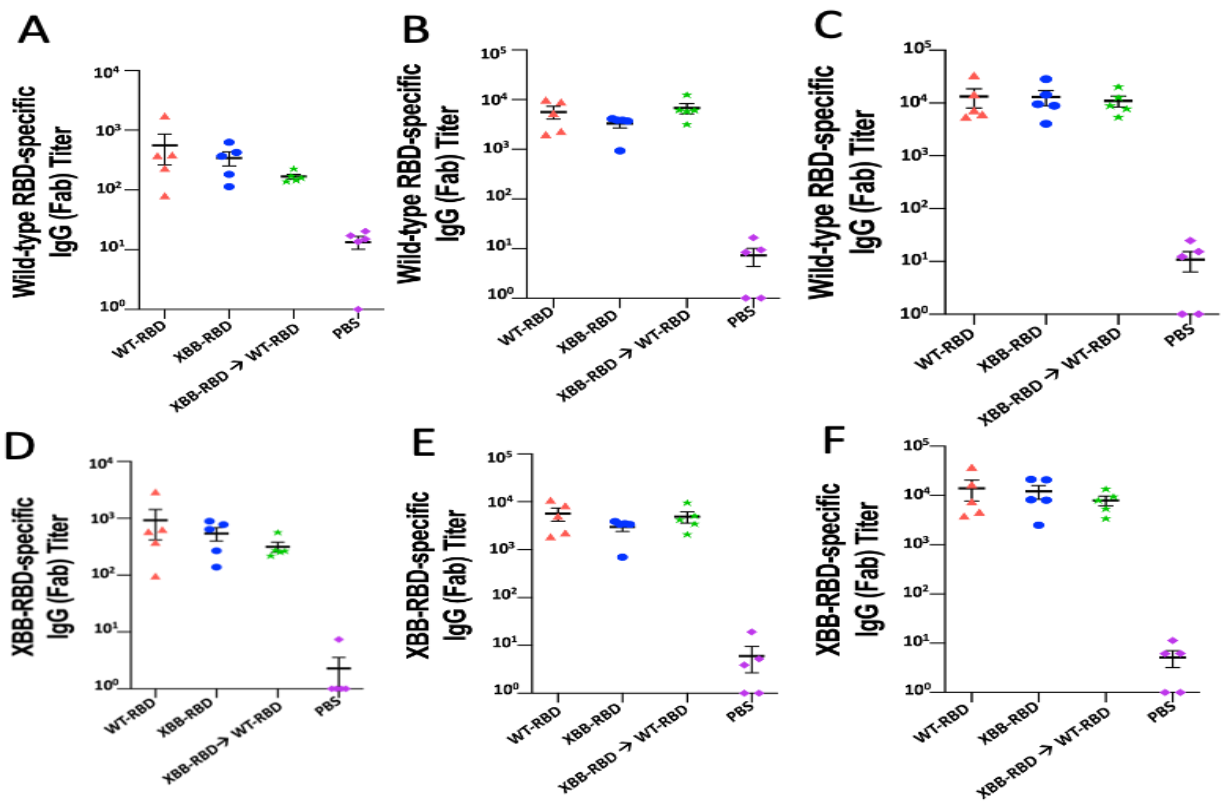

Figure 10: Titer of IgG (Fab) with 3 Different Sera from Different Time Points Specific to Each Protein.
A) SARS-CoV-2 wild-type (WT)-RBD-specific IgG (Fab) titer for the first serum; B) SARS-CoV-2 WT-RBD-specific IgG (Fab) titer for the second serum; C) SARS-CoV-2 WT-RBD-specific IgG (Fab) titer for the third serum; D) SARS-CoV-2 XBB-RBD-specific IgG (Fab) titer for the first serum; E) SARS-CoV-2 XBB-RBD-specific IgG (Fab) for the second serum; F) SARS-CoV-2 XBB-RBD-specific IgG (Fab) titer for the third serum.

The second antibody studied was IgG full-length and the third serum was utilized. Figure 11 shows similar results to the IgG Fab portion. The three protein-based vaccines induced high IgG full-length titers, while the PBS control group induced background levels.

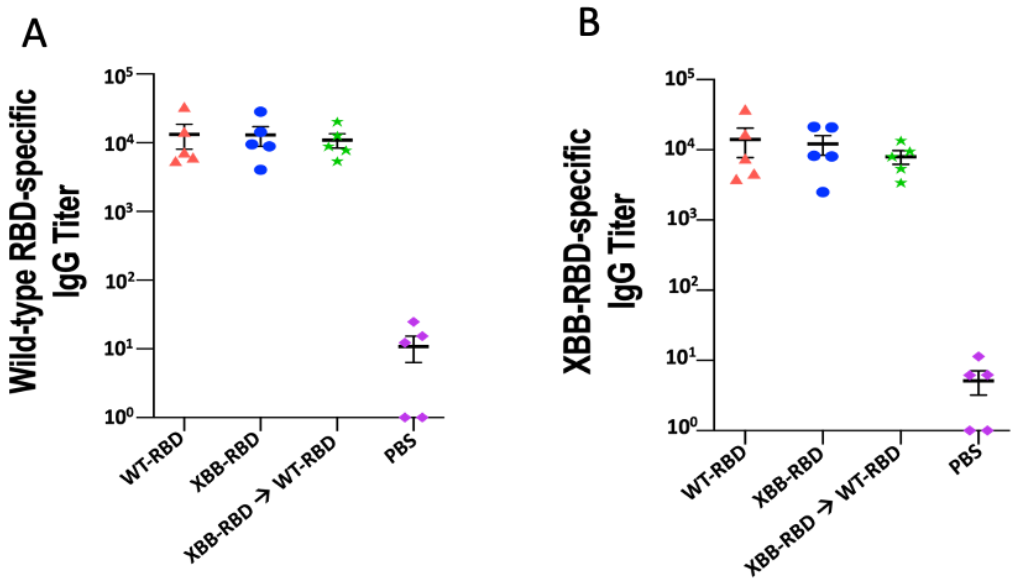

Figure 11: Titer of IgG Full-Length Specific to Each Protein.
A) SARS-CoV-2 wild-type (WT)-RBD-specific IgG full-length titer for the third serum; B) SARS-CoV-2 XBB-RBD-specific IgG full-length titer for the third serum.

Titers of IgG subtypes IgG1 and IgG2a were tested due to each subtype being involved in a different mechanism. IgG1 is linked to a type 2 helper (Th2) response and IgG2a is linked to a type 1 helper (Th1) response (31). IgG1 subtype induced a slightly higher titer for both wild-type and mutant-specific proteins compared to IgG2a. In all cases, the protein-specific vaccination groups induced a high-level titer while PBS only induced background levels. The IgG1/IgG2a ratio was calculated for each individual mouse and then averaged. For wild-type RBD-specific subtypes, the vaccinated group wild-type-RBD induced a more balanced ratio. For XBB-RBD-specific subtype antibodies, the vaccinated group XBB-RBD induced a more balanced ratio. Overall, all groups had an even ratio, which implies that there is even amount of Th1 and Th2 responses to the protein antigens.

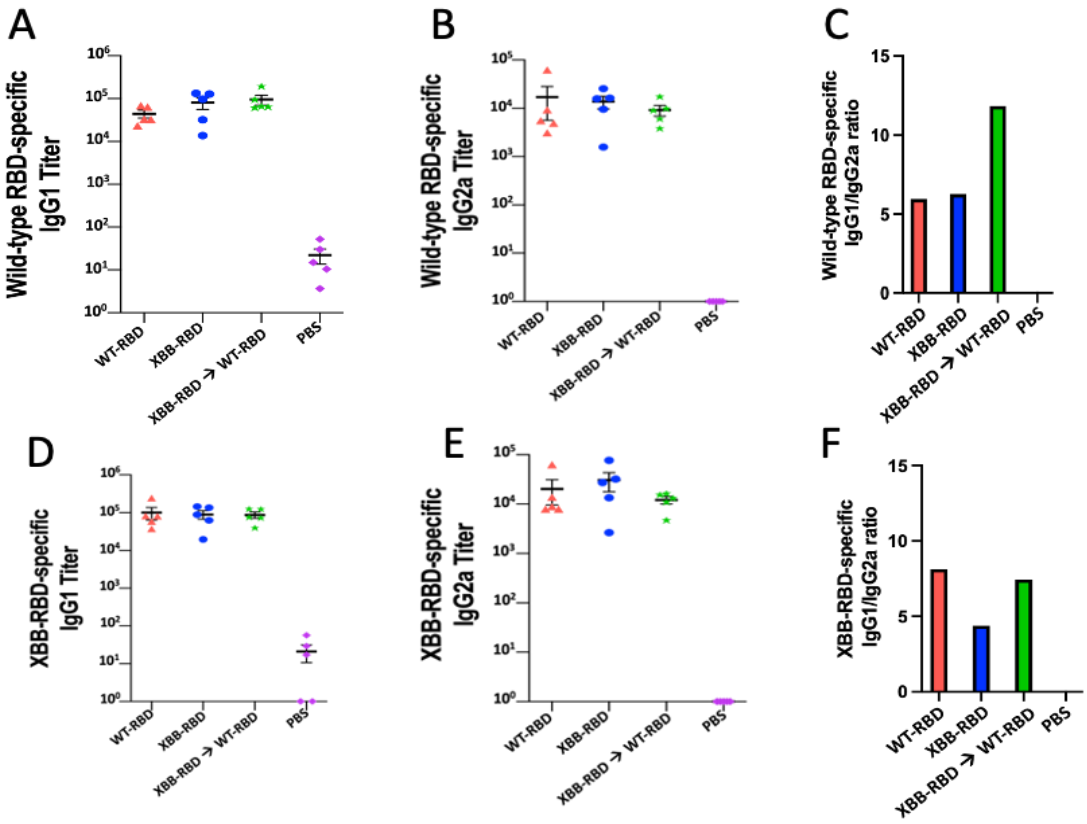

Figure 12: Titer for IgG Subtypes Specific to Each Protein and IgG1/IgG2a Ratio.
A) SARS-CoV-2 wild-type (WT)-RBD-specific IgG1 titer for the third serum; B) SARS-CoV-2 WT-RBD-specific IgG2a titer for the third serum; C) SARS-CoV-2 WT-RBD-specific IgG1/IgG2a ratio; D) SARS-CoV-2 XBB-RBD-specific IgG1 titer for the third serum; E) SARS-CoV-2 XBB-RBD-specific IgG2a titer for the third serum; F) SARS-CoV-2 XBB-RBD-specific IgG1/IgG2a ratio.

Data for the neutralization assay against wild-type strain was gifted for this study. The sera used for the study was the 3rd collection (post-second boost). Both WT-RBD (SARS-CoV-2 wild-type-RBD) and the XBB-RBD to WT-RBD (prime: XBB-RBD & 2 boosts: WT-RBD) induced a high neutralizing antibody titer compared to the XBB-RBD. The XBB-RBD and PBS induced no neutralizing antibody activity against the original strain of SARS-CoV-2.

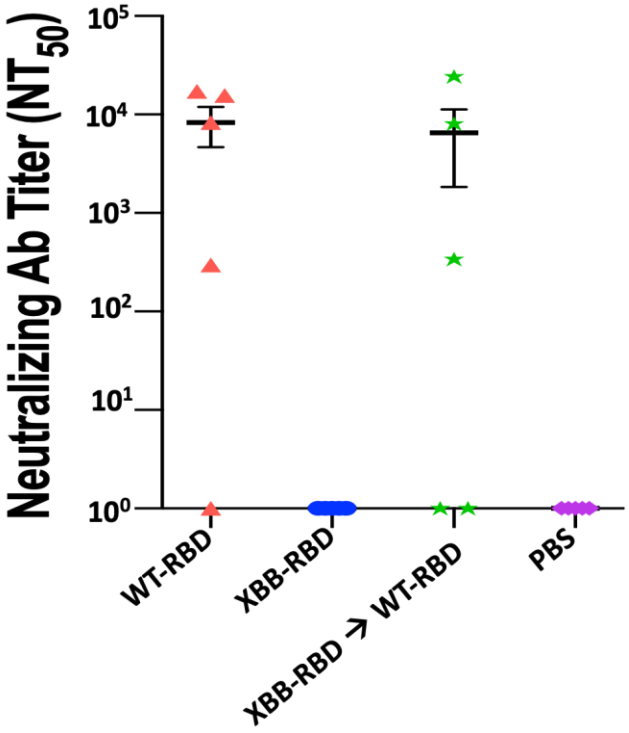

Figure 13: Neutralizing Antibody Titer Against Original SARS-CoV-2 Strain.

5. Discussion

The three protein vaccine groups induced a high-titer immune response, which potentially attributed to glycosylation, attachment of the Fc portion of IgG, and inclusion of the adjuvant Poly (I:C). Previous studies have demonstrated the enhanced efficacy of vaccines through these modifications or optimization of the adjuvant. Poly (I:C) is a synthetic double-stranded RNA polymer that has been successfully used as an adjuvant for mucosal vaccines (32). The receptor for Poly (I:C) is toll-like receptor 3 (TLR3) and induces type 1 interferon (33). It has been optimized in the lab's previous mucosal studies, resulting in a robust systemic and mucosal immunity by inducing IgA antibody.

In comparing the antibody titer of IgG Fab portion among the sera induced by one to three doses, the results suggest that a second booster may not be necessary to induce a high

RBD-specific titer. Although a slightly higher titer was induced from the third sera, the difference was not substantial between the third sera and second sera. Further studies are warranted to conclusively determine the necessity of a second booster. If studies continue to support the efficacy of two-dose administration, this could be perceived as favorable among the population due to eliminating the need for frequent vaccinations.

When the ratio of vaccine-induced IgG1 and IgG2a is not balanced, it could cause inflammation, which can lead to side effects, such as fever, fatigue, and headache (34). Therefore, balanced IgG1/IgG2a ratios are necessary to prevent inflammation. Here, we demonstrated the overall balanced ratio of IgG1 and IgG2a subtype antibodies induced by both wild-type-RBD and XBB-RBD proteins among all three different vaccinations groups, indicating that the immune system does not potentially cause an inflammatory reaction to the vaccines.

In this study, two vaccination groups, including wild-type-RBD and its prime with the XBB-RBD, induced an effective neutralizing titer against the wild-type strain after intranasal immunization. By contrast, the XBB-RBD on its own did not induce neutralizing antibodies against the wild-type strain. This data is consistent with previous studies, showing reduced neutralizing antibodies induced by vaccines targeting other Omicron subvariants such as BA.1 against the original viral strain (35). While evaluation of the neutralizing activity of these vaccines, particularly XBB-RBD, against the Omicron variants is ongoing, it is anticipated that XBB-RBD subunit vaccine will induce effective neutralizing antibodies against Omicron variants, but its prime vaccination with wild-type RBD will elicit effective neutralizing antibodies against both wild-type strain and Omicron variants. With further studies, a bivalent vaccine, particularly prime-boost vaccines (consisting of the variant and wild-type RBDs), may hold promise as a

more effective candidate with neutralizing activity against wild-type strain and different variants.

6. Conclusion and Future Direction

The overall purpose of this study is to develop a mucosal vaccine utilizing the RBD portion of the SARS-CoV-2 spike protein to induce localized nasal immunity and broad-spectrum neutralizing antibody response. The aim is to also create a mucosal vaccine to induce immunity for both previous and emerging COVID-19 variants. The route of infection for COVID-19 starts within the respiratory pathway and it is important to create a first line of defense within the nasal mucosal surfaces to prevent the binding and replication of COVID-19.

Previous studies from our lab have shown that wild-type-RBD or Delta-RBD protein-based subunit vaccines that are glycosylated and tagged with the Fc portion of the IgG produce high-level antibody responses via the intramuscular or intranasal route, which provide protection against wild-type and different variants (28). In this study, all three vaccination groups, which are based on the glycosylated XBB-RBD or its prime vaccination with the wild-type-RBD, induced a high-level RBD-specific IgG antibody responses and subtype antibodies via the mucosal route.

Mucosal surfaces provide immunity through mucosal IgA antibody. Future studies will assess the titer of vaccine-induced IgA antibody by sacrificing mice to collect the BAL. The generated vaccines are expected to provide localized immunity by induction of strong IgA antibody response. Further studies will also challenge the intranasally immunized mice with SARS-CoV-2 variants to evaluate the vaccine's immunity in protecting animals from variant infection.

Overall, the vaccines that were designed and studied here have the potential to be developed as an effective mucosal vaccine via the intranasal route, being capable of neutralizing divergent SARS-CoV-2 strains with protective efficacy against current and future emerging variants. The long-term goal with these vaccines is to prevent infections, hospitalizations, and deaths caused by COVID-19.

REFERENCES

1. World Health Organization. (2023). Who coronavirus (COVID-19) dashboard. https://covid19.who.int/.
2. Pal, M., Berhanu, G., Desalegn, C., & Kandi, V. (2020). Severe acute respiratory syndrome coronavirus-2 (SARS-CoV-2): An Update. *Cureus*. https://doi.org/10.7759/cureus.7423.
3. Saravanan, K. A., Panigrahi, M., Kumar, H., Rajawat, D., Nayak, S. S., Bhushan, B., & Dutt, T. (2022). Role of genomics in combating COVID-19 pandemic. *Gene*, *823*, 146387. https://doi.org/10.1016/j.gene.2022.146387.
4. Satarker, S., & Nampoothiri, M. (2020). Structural proteins in severe acute respiratory syndrome coronavirus-2. *Archives of Medical Research*, *51*(6), 482–491. https://doi.org/10.1016/j.arcmed.2020.05.012.
5. Yang, Y., & Du, L. (2021). SARS-CoV-2 spike protein: A key target for eliciting persistent neutralizing antibodies. *Signal Transduction and Targeted Therapy*, *6*(1). https://doi.org/10.1038/s41392-021-00523-5.
6. Wang, N., Shang, J., Jiang, S., & Du, L. (2020). Subunit vaccines against emerging pathogenic human coronaviruses. *Frontiers in Microbiology*, *11*. https://doi.org/10.3389/fmicb.2020.00298.
7. Guan, X., Yang, Y., & Du, L. (2023). Advances in SARS-CoV-2 receptor-binding domain-based COVID-19 vaccines. *Expert Review of Vaccines*, *22*(1), 422–439. https://doi.org/10.1080/14760584.2023.2211153.

8. Huang, Y., Yang, C., Xu, X., Xu, W., & Liu, S. (2020). Structural and functional properties of SARS-CoV-2 spike protein: Potential antivirus drug development for COVID-19. *Acta Pharmacologica Sinica*, *41*(9), 1141–1149. https://doi.org/10.1038/s41401-020-0485-4.

9. Shirbhate, E., Pandey, J., Patel, V. K., Kamal, M., Jawaid, T., Gorain, B., Kesharwani, P., & Rajak, H. (2021). Understanding the role of ACE-2 receptor in pathogenesis of COVID-19 disease: A potential approach for therapeutic intervention. *Pharmacological Reports*, *73*(6), 1539–1550. https://doi.org/10.1007/s43440-021-00303-6.

10. V'kovski, P., Kratzel, A., Steiner, S., Stalder, H., & Thiel, V. (2020). Coronavirus biology and replication: Implications for SARS-CoV-2. *Nature Reviews Microbiology*, *19*(3), 155–170. https://doi.org/10.1038/s41579-020-00468-6.

11. Malone, B., Urakova, N., Snijder, E. J., & Campbell, E. A. (2021). Structures and functions of coronavirus replication–transcription complexes and their relevance for SARS-CoV-2 drug design. *Nature Reviews Molecular Cell Biology*, *23*(1), 21–39. https://doi.org/10.1038/s41580-021-00432-z.

12. Wu, W., Cheng, Y., Zhou, H., Sun, C., & Zhang, S. (2023). The SARS-CoV-2 nucleocapsid protein: Its role in the viral life cycle, structure and functions, and use as a potential target in the development of vaccines and diagnostics. *Virology Journal*, *20*(1). https://doi.org/10.1186/s12985-023-01968-6.

13. Clausen, T. M., Sandoval, D. R., Spliid, C. B., Pihl, J., Perrett, H. R., Painter, C. D., Narayanan, A., Majowicz, S. A., Kwong, E. M., McVicar, R. N., Thacker, B. E., Glass, C. A., Yang, Z., Torres, J. L., Golden, G. J., Bartels, P. L., Porell, R. N., Garretson, A. F., Laubach, L., Feldman, J., Yin, X., Pu, Y., Hauser B. A., Caradonna, T. M., Kellman, B. P., Martino, C., Gordts, P. L. S. M.,

Chanda, S. K., Schmidt, A. G., Godula, K., Leibel, S. L., Jose, J., Corbett, K. D., Ward, A. B., Carlin, A. F., & Esko, J. D. (2020). SARS-CoV-2 infection depends on cellular heparan sulfate and ACE2. *Cell*, *183*(4). https://doi.org/10.1016/j.cell.2020.09.033.

14. Carabelli, A. M., Peacock, T. P., Thorne, L. G., Harvey, W. T., Hughes, J., de Silva, T. I., Peacock, S. J., Barclay, W. S., de Silva, T. I., Towers, G. J., & Robertson, D. L. (2023). SARS-CoV-2 variant biology: Immune escape, transmission and fitness. *Nature Reviews Microbiology*. https://doi.org/10.1038/s41579-022-00841-7.
15. Ao, D., Lan, T., He, X., Liu, J., Chen, L., Baptista-Hon, D. T., Zhang, K., & Wei, X. (2022). SARS-CoV-2 omicron variant: Immune Escape and vaccine development. *MedComm*, *3*(1). https://doi.org/10.1002/mco2.126.
16. Hao, Y., Wang, Y., Wang, M., Zhou, L., Shi, J., Cao, J., & Wang, D. (2022). The origins of COVID-19 pandemic: A brief overview. *Transboundary and Emerging Diseases*, *69*(6), 3181–3197. https://doi.org/10.1111/tbed.14732.
17. World Health Organization. (2021). Coronavirus disease (COVID-19): How is it transmitted. https://www.who.int/news-room/questions-and-answers/item/coronavirus-disease-covid-19-how-is-it-transmitted.
18. Bar-On, Y. M., Flamholz, A., Phillips, R., & Milo, R. (2020). SARS-CoV-2 (COVID-19) by the numbers. *eLife*, *9*. https://doi.org/10.7554/elife.57309.
19. Johns Hopkins Coronavirus Resource Center. (2023). Mortality analyses. https://coronavirus.jhu.edu/data/mortality.

20. Rahman, Md. M., Masum, Md. H., Wajed, S., & Talukder, A. (2022). A comprehensive review on COVID-19 vaccines: Development, effectiveness, adverse effects, distribution and challenges. *VirusDisease*, *33*(1), 1–22. https://doi.org/10.1007/s13337-022-00755-1.

21. Zieneldien, T., Kim, J., Cao, J., & Cao, C. (2021). COVID-19 vaccines: Current conditions and future prospects. *Biology*, *10*(10), 960. https://doi.org/10.3390/biology10100960

22. Centers for Disease Control and Prevention. (2023). Overview of COVID-19 vaccines. https://www.cdc.gov/coronavirus/2019-ncov/vaccines/different-vaccines/overview-COVID-19-vaccines.html.

23. Fang, E., Liu, X., Li, M., Zhang, Z., Song, L., Zhu, B., Wu, X., Liu, J., Zhao, D., & Li, Y. (2022). Advances in COVID-19 mRNA vaccine development. *Signal Transduction and Targeted Therapy*, *7*(1). https://doi.org/10.1038/s41392-022-00950-y.

24. FDA. (2023). FDA takes action on updated mRNA COVID-19 vaccines to better protect against currently circulating variants. U.S. Food and Drug Administration. https://www.fda.gov/news-events/press-announcements/fda-takes-action-updated-mrna-covid-19-vaccines-better-protect-against-currently-circulating#:~:text=Today%27s%20actions%20relate%20to%20updated,the%20Omicron%20variant%20XBB.1.5.

25. Kehagia, E., Papakyriakopoulou, P., & Valsami, G. (2023). Advances in intranasal vaccine delivery: A promising non-invasive route of immunization. *Vaccine*, *41*(24), 3589–3603. https://doi.org/10.1016/j.vaccine.2023.05.011

26. Afkhami, S., D'Agostino, M. R., Zhang, A., Stacey, H. D., Marzok, A., Kang, A., Singh, R., Bavananthasivam, J., Ye, G., Luo, X., Wang, F., Ang, J. C., Zganiacz, A., Sankar, U., Kazhdan, N., Koenig, J. F. E., Phelps, A., Gameiro, S. F., Tang, S., … Xing, Z. (2022). Respiratory mucosal delivery of next-generation COVID-19 vaccine provides robust protection against both ancestral and variant strains of SARS-CoV-2. *Cell*, *185*(5). https://doi.org/10.1016/j.cell.2022.02.005.

27. Du, Y., Xu, Y., Feng, J., Hu, L., Zhang, Y., Zhang, B., Guo, W., Mai, R., Chen, L., Fang, J., Zhang, H., & Peng, T. (2021). Intranasal administration of a recombinant RBD vaccine induced protective immunity against SARS-CoV-2 in mouse. *Vaccine*, *39*(16), 2280–2287. https://doi.org/10.1016/j.vaccine.2021.03.006.

28. Shi, J., Zheng, J., Tai, W., Verma, A. K., Zhang, X., Geng, Q., Wang, G., Guan, X., Malisheni, M. M., Odle, A. E., Zhang, W., Li, F., Perlman, S., & Du, L. (2022). A glycosylated RBD protein induces enhanced neutralizing antibodies against Omicron and other variants with improved protection against SARS-CoV-2 infection. *Journal of Virology*, *96*(17). https://doi.org/10.1128/jvi.00118-22.

29. Portolano, N., Watson, P. J., Fairall, L., Millard, C. J., Milano, C. P., Song, Y., Cowley, S. M., & Schwabe, J. W. R. (2014). Recombinant protein expression for structural biology in HEK 293F suspension cells: A novel and accessible approach. *Journal of Visualized Experiments*, (92). https://doi.org/10.3791/51897.

30. Vidarsson, G., Dekkers, G., & Rispens, T. (2014). IgG subclasses and allotypes: From structure to effector functions. *Frontiers in Immunology*, *5*. https://doi.org/10.3389/fimmu.2014.00520.

31. Bretscher, P. (2019). On analyzing how the Th1/Th2 phenotype of an immune response is determined: Classical observations must not be ignored. *Frontiers in Immunology*, *10*. https://doi.org/10.3389/fimmu.2019.01234.

32. Ma, C., Li, Y., Wang, L., Zhao, G., Tao, X., Tseng, C.-T. K., Zhou, Y., Du, L., & Jiang, S. (2014). Intranasal vaccination with recombinant receptor-binding domain of MERS-CoV spike protein induces much stronger local mucosal immune responses than subcutaneous immunization: Implication for designing novel mucosal MERS Vaccines. *Vaccine*, *32*(18), 2100–2108. https://doi.org/10.1016/j.vaccine.2014.02.004.

33. Matsumoto, M., & Seya, T. (2008). TLR3: Interferon induction by double-stranded RNA including Poly(I:C). *Advanced Drug Delivery Reviews*, *60*(7), 805–812. https://doi.org/10.1016/j.addr.2007.11.005.

34. Hervé, C., Laupèze, B., Del Giudice, G., Didierlaurent, A. M., & Tavares Da Silva, F. (2019). The how's and what's of vaccine reactogenicity. *Npj Vaccines*, *4*(1). https://doi.org/10.1038/s41541-019-0132-6.

35. Shi, J., Wang, G., Zheng, J., Verma, A. K., Guan, X., Malisheni, M. M., Geng, Q., Li, F., Perlman, S., & Du, L. (2022). Effective vaccination strategy using SARS-CoV-2 spike cocktail against Omicron and other variants of concern. *Npj Vaccines*, *7*(1). https://doi.org/10.1038/s41541-022-00580-z.

VITAE

MELISSA LIZBETH PALACIOS

EDUCATION

Georgia State University
Atlanta, GA
August 2022
Expected Graduation Date: December 2023

Master of Interdisciplinary Studies Biomedical Sciences Enterprise
Research Thesis: SARS-CoV-2 Receptor-Binding Domain-Based Mucosal COVID-19 Vaccines

Kennesaw State University
Kennesaw, GA

August 2015 - May 2019
Bachelor of Science in Biology
Clubs: American Medical Student Association

RELEVANT COURSEWORK

- Immunology
- Virology
- Toxicology
- Human Physiology
- Microbiology
- Cell Biology
- Biostatistics
- Biochemistry

RESEARCH

August 2022-Present
Atlanta, GA

Working under Dr. Lanying Du at Georgia State University. Using different techniques such as ELISA, PCR, plasmid amplification, plasmid purification, protein purification, etc. for vaccine studies of COVID-19. Have experience working with mice in animal biosafety level -2.

August 2017 - May 2019
Kennesaw, GA

Worked under Dr. Alyssa Gulledge and Dr. Thomas McElroy at Kennesaw State University. Attempted to identify at what stage a scorpion's (*Centruroides vittatus)* life changes its gene expression to have a more toxic venom. DNA was isolated from the telson of different class sizes of scorpions after releasing their venom. Primer sequences were produced in silico to be able to isolate amplicon for toxin proteins. Different laboratory techniques were performed – DNA isolation, polymerase chain reaction, quantitative polymerase chain reaction, and gel electrophoresis.

May 2016 - July 2017
Kennesaw, GA

Worked under master's student Margaret Aduddell and Dr. Thomas McElroy at Kennesaw State University. Studied how forest restoration through fire burning affects the bat community. Bat activity was monitored by deploying bat detectors throughout the forest. Their activity was also monitored through their diet. Insects were collected throughout the bats' habitat during the night in buckets, which later were stored in ethanol to then be sorted by order. Different methods were found through reading scientific literature.

WORK/VOLUNTEER EXPERIENCE

Cryolife, Inc.
Kennesaw, GA
September 2019 - Current
Cardiac Dissector

Dissect and process cardiovascular tissue in a timely manner prior to the expiration. Maintain a high yield of 76.9% and high feedback of 2.2 out of 3 on tissue. Received a core behavior award for the second quarter of 2020 for results driven. Train other team members unfamiliar with heart dissections. Teach them different techniques and attributes of the aorta and pulmonary valves. Inspect cardiac tissue processed by dissectors to provide quality tissue to patients and make sure doctors know the right measurements and attributes.

Cobb and Douglas Public Health Department
Marietta, GA
August 2020 - March 2021
Case Investigator

Informed recently tested COVID-19 positive cases of their results. Educate patients on the proper isolation period. Gather patients' information including demographics, occupation, and close contacts for contact tracing. Follow HIPAA compliance laws while talking to the patients. Took several training courses such as the Johns Hopkins University COVID-19 Contact Tracing course and National Network of Disease Intervention Training Centers (NNDITC) Case Investigating course. Under a grant, tested samples for COVID-19 at the medical examiner's office.

Emory Clinic
Atlanta, GA
January 2018 - August 2018
Volunteer Tech

Served multiple roles in the clinic to aid staff and to patients. Worked front desk for multiple departments and guided patients to accurate location of their appointment. Directly helped the Department of Urology with creating starter packets and sterilizing patient beds during heavy patient flow.

Gustafson Chiropractic
Sandy Springs, GA
June 2015 - November 2016
Chiropractic Assistant

Assisted the chiropractor in secondary needs. Administered therapies for patients. Accurately gathered information of the patient regarding their car accident. With the information given by the patient, an accident report would made which included the patient's therapy course and overall improvement. Accident reports were made for legal purposes which would be sent to the patient's lawyer.